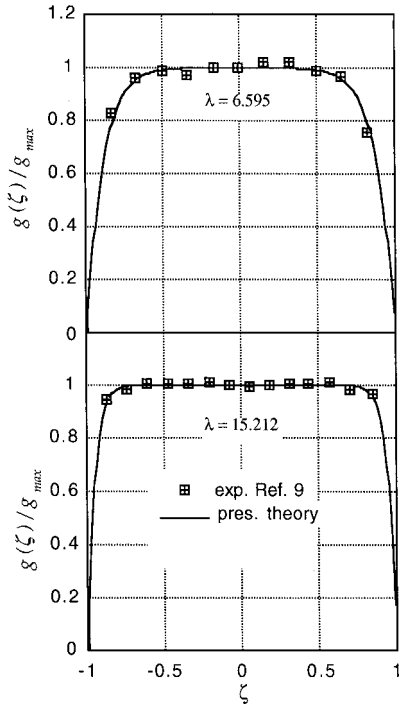

Fig. 3 Comparison of the experimental and theoretical velocity profiles for accelerating flows.

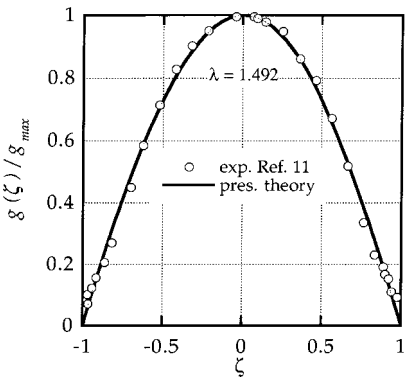

Fig. 4 Comparison of experimental and theoretical velocity profiles for decelerating flows.

measurements of Singh[9] for the case of an accelerating flow, whereas in Fig. 4 the measurements of Tabatabai and Pollard[11] for the decelerating flow are presented. It is clear that, in both cases, the present solution provides a reasonable approximation. It is also fair to say that the same degree of approximation to the accelerating flow can also be achieved via the finite differences, primitive variable, solution of Singh.[9] The latter method, however, involves the axisymmetric case of the Navier–Stokes equations and includes the effects of turbulence via the k–ε model.

Conclusions

The Note reported on numerical solutions of converging and diverging unidirectional flows. The solution to the problem was accomplished using a shooting method, whereby the governing equation was written as a system of three nonlinear first-order ODEs and was solved as an initial value problem via the Runge–Kutta method. The results of the numerical study are shown to compare well with the experimental measurements. The present simple method provided equivalent findings with the previously reported analysis that uses mathematically cumbersome elliptic integrals.

References

[1]Murphy, H. D., Chambers, F. W., and McEligot, D. M., "Laterally Converging Flow. Part 1. Mean Flow," *Journal of Fluid Mechanics*, Vol. 127, 1983, pp. 379–401.

[2]Mochizuki, S., and Yang, W.-Y., "Self-Sustained Radial Oscillating Flows Between Parallel Disks," *Journal of Fluid Mechanics*, Vol. 154, 1985, pp. 377–397.

[3]Keller, H. B., *Numerical Methods for Two-Point Boundary Value Problems,* Ginn-Blaisdell, Waltham, MA, 1968, pp. 39–61.

[4]Vatistas, G. H., and Ghaly, S. G., "On the Pure Polar Flow Within Two Concentric Spheres," *International Journal of Computers and Fluids*, Vol. 26, No. 7, 1997, pp. 683–695.

[5]Vatistas, G. H., and Ghaly, W. S., "Converging and Diverging Flow in Narrow Conical Passages," *Acta Mechanica*, Vol. 136, June 1999, pp. 209–222.

[6]Zitouni, G., and Vatistas, G. H., "Purely Accelerating and Decelerating Flows within Two Flat Disks," *Acta Mechanica*, Vol. 123, 1996, pp. 151–161.

[7]Isaacson, E., and Keller, H. B., *Analysis of Numerical Methods,* Wiley, New York, 1966, pp. 424–427.

[8]Hayes, W. F., and Tucker, H. G., "Theoretical Radial Pressure Distribution for Viscous Fluid Inflow within a Thin Disk Chamber," National Research Council of Canada, Rept. NRC-CS-51, Ottawa, ON, Canada, 1973.

[9]Singh, A., "Theoretical and Experimental Investigations on Inward Flow Between Two Disks," Ph.D. Dissertation, Dept. of Mechanical Engineering, Indian Inst. of Technology, Bombay, India, 1993.

[10]Moller, P. S., "Radial Flow without Swirl Between Parallel Disks," *Aeronautical Quarterly*, Vol. 14, 1963, pp. 163–185.

[11]Tabatabai, M., and Polard, A., "Turbulence in Radial Flow Between Parallel Disks at Medium and Low Reynolds Numbers," *Journal of Fluid Mechanics*, Vol. 185, 1987, pp. 483–502.

P. R. Bandyopadhyay
Associate Editor

Examination of Anomalous Shock Velocities in Weakly Ionized Gases

B. Shirinzadeh,* G. C. Herring,† and R. J. Exton*
NASA Langley Research Center,
Hampton, Virginia 23681-2199

Introduction

RECENT studies (see Ref. 1 for a review) subtly suggest that new physics may be necessary to explain anomalous drag reduction and shock propagation in a weakly ionized gas (WIG). Several[2–6] studies conclude that shock waves travel faster in the WIG (fractional ionization $\sim 10^{-6}$) than expected from the gas temperature. Other work[7] concludes that anomalous dispersion and attenuation effects cannot be explained only with thermal effects. More recent work (Ref. 8 and references therein) has alternatively argued that temperature gradients and viscous effects in the discharge can explain the shock dispersion, splitting, and attenuation. In this Note, we address the issue of shock speeds and argue that the measured shock speeds are not anomalous. Using standard one-dimensional and inviscid normal shock wave gasdynamics, we use the experimental parameters provided in these studies to show that the observed shock wave speeds are the same as those expected for the given temperatures.

Description

In these experiments, a steady WIG discharge is produced in a localized region of a low-pressure tube, in which the pressures

Received 20 March 2000; revision received 23 January 2001; accepted for publication 22 February 2001.

*Aerospace Technologist, Advanced Measurement Diagnostics Branch, M/S 493.

†Aerospace Technologist, Advanced Measurement Diagnostics Branch, M/S 493. Member AIAA.

of the hotter WIG and the surrounding colder neutral gas, that is, un-ionized, are equal. The spark-initiated shocks are formed in the neutral gas and allowed to propagate into the WIG. In some of these studies,[2,7] the interface between the neutral gas and the WIG is assumed to be a contact surface, that is, tangential discontinuity, to analyze the problem. Thus, we first predict WIG shock speeds, assuming that the interface is a contact surface. In this case, the interface reflects part of the incident shock energy into the neutral gas, and the energy of the shock transmitted into the WIG is reduced, relative to the incident shock energy. However, for a steady discharge in a constant-pressure cell, an alternative assumption for the WIG–neutral interface is a continuous transition that extends over a finite distance along the tube axis. In this case, the reflected wave is negligible, and the shock energy transmitted into the WIG is equal to the incident shock energy. We also predict WIG shock speeds using this second model. Finally, we show that measurements from these studies[2–7] support our assumption that the shock energy in the WIG, ΔQ_p, is about the same as the incident shock energy in the neutral gas, ΔQ_0.

Results

We first review the results of Refs. 2–5 and 7. Reference 6 is not included because it does not give the temperature of the WIG. Reference 4 gives temperatures and shock speeds for two locations; we use the on-axis $x = 0$ data. Table 1 summarizes the data for the neutral gas. Subscript 0 denotes neutral-gas values in front of the shock, whereas subscript 1 denotes neutral-gas values behind the shock. The reported gas temperature T_0 and shock speed V_0 are used to calculate the speed of sound S_0 and the Mach number M_0 of the shock wave. References 3 and 7 explicitly give $T_0 = 293$ and 300 K, respectively; the other references imply room temperature. We arbitrarily use 293 K for Refs. 2, 4, and 5. Using M_0, we obtain the temperature (T_1/T_0) and density (ρ_1/ρ_0) jumps across the shock from standard treatments of inviscid, one-dimensional, normal shock analysis. If γ is the ratio of specific heats, these jumps are[9]

$$\rho_1/\rho_0 = M_0^2(\gamma+1)\Big/\left[M_0^2(\gamma-1)+2\right]$$

$$T_1/T_0 = \left[M_0^2(\gamma-1)+2\right]\left[2\gamma M_0^2-(\gamma-1)\right]\Big/[M_0(\gamma+1)]^2$$

The energy density ΔQ that created the shock wave is the same as the difference in the total (internal plus kinetic) energy density, before and after the shock. From the Rankine–Hugoniot relations, one can show that the difference in total energy per unit volume is proportional to $\rho\Delta T$. Thus, $\Delta Q_0 \propto \rho_0(T_1 - T_0)$. In the last row of Table 1, we have tabulated this estimate of the energy necessary to sustain the shock in the neutral gas. This energy is in degrees Kelvin times the initial density ρ_0 in front of the shock.

Table 2 summarizes the measured shock speeds V_p in the WIG, which are supposedly too large for the given temperatures T_p. For Ref. 7, we use the 50-mA data. Subscript p denotes values in the plasma in front of the shock wave, whereas subscript 2 denotes values in the plasma behind the shock. We use T_p to calculate the sound speed S_p and Mach number M_p of the shock in the discharge. Again, the normal shock relations are used to calculate the temperature and density jumps across the shock. In the last row, $\Delta Q_p \propto \rho_p(T_2 - T_p)$ is used to list the energy to sustain the shock in the WIG plasma.

Table 1 Measured shock wave speeds V_0 and related parameters in neutral gases

	Reference				
Parameter	2	3	4	5	7
Gas	Air	Air	Argon	Air	Air
T_0, K	293	293	293	293	300
S_0, m/s	343	343	319	343	347
V_0, m/s	700	416	523	650	515
M_0	2.04	1.21	1.64	1.9	1.48
ΔQ_0, K $\cdot \rho_0$	$211\rho_0$	$38\rho_0$	$190\rho_0$	$179\rho_0$	$93\rho_0$

Table 2 Measured shock wave speeds V_p and related parameters in WIG

	Reference				
Parameter	2	3	4	5	7
T_p, K	2000	1250	1050	1000	543
S_p, m/s	896	708	604	634	467
V_p, m/s	1900	850	886	1250	653
M_p	2.12	1.20	1.47	1.97	1.4
ΔQ_p, (K $\cdot \rho_0$)	$231\rho_0$	$38\rho_0$	$135\rho_0$	$193\rho_0$	$78\rho_0$

Using two different models of the neutral–WIG interface to predict the WIG shock speed, we now argue that the measured WIG shock velocities of Table 2 are about what we expect for the reported temperatures T_p. Both models assume that pressure, specific heat, and γ do not vary from the WIG to the neutral gas and that viscosity and heat conduction are negligible. Additionally, a steady shock is assumed in both models.

In the first model, we assume that the interface between the cold neutral gas and the hot plasma is abrupt, that is, a contact surface. This problem is well known.[9] Pressure and gas velocity are constant over the interface, whereas temperature and density are discontinuous. A fraction of the incident shock energy is transmitted as a weaker shock into the WIG, while the remaining energy is reflected into the neutral gas as a rarefaction wave. The amount of energy transmitted depends on the magnitude of the density decrease at the interface. The Mach number M_R of the transmitted shock is given by[10]

$$M_0\left(1-1/M_0^2\right)+\{M_0(\gamma-1)\}^{-1}\left\{\left[2\gamma M_0^2-(\gamma-1)\right]\times\left[(\gamma-1)M_0^2+2\right]\right\}^{\frac{1}{2}}\left\{1-\left[\left[2\gamma M_R^2-(\gamma-1)\right]\Big/\left[2\gamma M_0^2-(\gamma-1)\right]\right]^{(\gamma-1)/2\gamma}\right\}=M_R(T_p/T_0)^{\frac{1}{2}}\left(1-1/M_R^2\right)$$

The Mach number M_R and shock velocity V_R (given in Table 3) are calculated by using M_0, T_0, and T_p from Tables 1 and 2. Subscript R denotes predicted values using this reflected rarefaction wave model. The fractional differences $(V_R - V_p)/V_p$ vary from 0.3 to +30% and are shown in Table 4. We believe these differences indicate reasonable agreement considering the uncertainties expected in the shock speed and WIG temperature measurements, as well as the pulse-to-pulse fluctuations in the electrical discharge energy of the shock-forming spark.

In the second model for predicting the shock speeds in the WIG, we assume an interface between the hot and cold gases that is smooth and extends over a finite distance along the tube axis. Again, pressure and gas velocity are constant over the interface, but temperature and density change in a continuous manner. In this case, there is no reflected wave. Thus, ΔQ_0 of the shock in the neutral gas is the same as ΔQ_p of the shock in the discharge. With the ideal gas law and the normal shock relations, one can show that the Mach numbers are equal. Thus, we explicitly equate the WIG Mach number to the neutral-gas Mach number and use subscript N to denote predicted shock values in the discharge under this condition. Thus, $M_N = M_0$,

Table 3 Summary of our predictions V_R with a reflected rarefaction wave, our predictions V_N with no reflected wave, predictions V_x from original works, and measurements from the original works V_p

	Reference				
Parameter	2	3	4	5	7
V_R, m/s	1328	804	856	1005	655
V_N, m/s	1828	857	991	1205	691
V_x, m/s	1350	——[a]	590	900	653
V_p, m/s	1900	850	886	1250	653

[a]Not quoted in original work.

Table 4 Comparison of velocities and shock energies

	Reference				
Parameter	2	3	4	5	7
$(V_R - V_p)/V_p$	−0.30	−0.05	−0.03	−0.20	0.003
$(V_n - V_p)/V_n$	−0.04	0.008	0.11	−0.04	0.06
$(\Delta Q_0 - \Delta Q_p)/\Delta Q_0$	−0.09	0	0.29	−0.08	0.16

that is, $\Delta Q_N = \Delta Q_0$. We then use the temperature T_p and sound speed S_p from Table 2 to calculate the expected no-reflection shock wave velocity V_N, with $V_N = M_N S_p \propto M_N (T_p)^{1/2}$. For this model, the overall agreement with measurement is noticeably better than for the first model. Comparing the predicted V_N in Table 3 to the observed V_p, we see in Table 4 differences that vary from 0.8 to 12%. We consider this agreement excellent, considering the expected errors in the measurements.

It is not surprising that the second model (no reflection) gives such good agreement with the measurements. After comparing the shocks in the neutral gas of Table 1 and the WIG of Table 2, the fractional differences $(\Delta Q_0 - \Delta Q_p)/\Delta Q_0$ are listed in Table 4. These differences are modest, being within the expected uncertainties mentioned earlier. Therefore, the data from the original studies show that $\Delta Q_0 \approx \Delta Q_p$. By exactly equating these energies in the second model, we are making only small changes to the experimental ΔQ_p that are already nearly equal.

The measurements V_p and the predictions V_x from the original studies, along with our two predictions (V_R and V_N), are summarized in Table 3. Our two models roughly agree with each other because the reflected wave of the first model is small for the temperatures T_p of Table 2. The relatively low T_p of Ref. 7 yields the smallest reflected wave, and so V_R and V_N differ the least, that is, 5%. The relatively high T_p for Ref. 2 produces the largest reflected wave, so that V_R and V_N differ the most, that is, 27%. In general, our two predictions (especially the no-reflection model) agree with the data V_p better than the original predictions V_x. The largest discrepancies between measurement and our predictions are 30 and 20% and occur for V_p and V_R of Refs. 2 and 5, but even these largest discrepancies are still within the uncertainty limits that we expect for the temperature measurements. The observed shock speeds are not significantly different from those calculated with the temperature of the WIG, using either model. Thus, we disagree with Refs. 2–6, which conclude that the measured shock speeds are too large compared to the predicted speeds based on thermal considerations. The good agreement between measurement and prediction, reported in Ref. 7, is consistent with our assertion that the shock speeds are not anomalous in a WIG.

Summary

In summary, using one-dimensional and inviscid gasdynamics, we conclude that the observed shock wave speeds agree with those expected from thermal heating. Additionally, Refs. 2–7 contain little discussion of the uncertainties for the shock wave speed and temperature measurements. It is important to determine the measurement uncertainties, including spatial and temporal inhomogeneities in the temperature of the WIG, before forming conclusions of anomalous shock effects. Finally, other reported WIG effects last for milliseconds[11] after the discharge is extinguished. Our estimated decay time to cool the WIG by thermal diffusion is also on the order of milliseconds. These similar times further suggest that the effects are thermal rather than plasma related. Based on the results of this Note and Refs. 8 and 11, we conclude that the observations[2–7] of shock wave speeds and dispersion can be explained with well-known fluid mechanics, the given gas temperature, temperature gradients, and viscosity.

References

[1] Hilbun, W. M., "Shock Waves in Nonequilibrium Gases and Plasmas," Ph.D. Dissertation, School of Engineering, U.S. Air Force Inst. of Technology, Wright–Patterson AFB, OH, 1997.

[2] Bytyurin, V., Klimov, A., Leonov, S., Lutsky, A., Van Wie, D., Brovkin, V., and Kolesnichenko, Y., "Effect of Heterogeneous Discharge Plasma on Shock Wave Structure and Propagation," AIAA Paper 99-4940, Nov. 1999.

[3] Basargin, I. V., and Mishin, G. I., "Probe Studies of Shock Waves in the Plasma of a Transverse Glow Discharge," *Soviet Technical Physics Letters*, Vol. 11, 1985, pp. 535–538.

[4] Basargin, I. V., and Mishin, G. I., "Shock-Wave Propagation in the Plasma of a Transverse Glow Discharge in Argon," *Soviet Technical Physics Letters*, Vol. 11, 1985, pp. 85–87.

[5] Klimov, A. I., Koblov, A. N., Mishin, G. I., Serov, Y. L., and Yavor, I. P., "Shock Wave Propagation in a Glow Discharge," *Soviet Technical Physics Letters*, Vol. 8, 1982, pp. 192–194.

[6] Ganguly, B. N., Bletzinger, P., and Garscadden, A., "Shock Wave Damping and Dispersion in Nonequilibrium Low Pressure Argon Plasmas," *Physics Letters A,* Vol. 230, June 1997, pp. 218–222.

[7] Bletzinger, P., and Ganguly, B. N., "Local Acoustic Shock Velocity and Shock Structure Recovery Measurements in Glow Discharges," *Physics Letters A*, Vol. 258, July 1999, pp. 342–348.

[8] White, A. R., Essenhigh, K. A., Adamovich, I., Lempert, W., and Subramaniam, V. V., "Effects of Thermal Gradients and Ionization on the Propagation of Spark-Generated Shock Waves," AIAA Paper 99-4855, Nov. 1999.

[9] Landau, L. D., and Lifshitz, E. M., *Fluid Mechanics*, Pergamon, Oxford, 1959, pp. 317–319, 331, 344–346, 353–366, 399–410.

[10] Aleksandrov, A. F., Vidyakin, N. G., Lakutin, V. A., Skvortsov, M. G., Timofeev, I. B., and Chernikov, V. A., "A Possible Mechanism for the Interaction of a Shock Wave with a Decaying Laser Plasma in Air," *Soviet Technical Physics Letters*, Vol. 31, 1986, pp. 468, 469.

[11] Klimov, A. I., Koblov, A. N., Mishin, G. I., Serov, Y. L., Khodataev, K. V., and Yavor, I. P., "Shock Wave Propagation in a Decaying Plasma," *Soviet Technical Physics Letters*, Vol. 8, 1982, pp. 240, 241.

M. Sichel
Associate Editor